Int J Interact Des Manuf (2007) 1:33–40
DOI 10.1007/s12008-007-0006-4

ORIGINAL PAPER

Detailed model of spot-welded joints to simulate the failure of car assemblies

Emmanuel H. J. Lamouroux · Daniel Coutellier · Norbert Doelle · Peter Kuemmerlen

Received: 1 October 2005 / Revised: 20 December 2005 / Accepted: 16 September 2006 / Published online: 16 March 2007

Abstract This paper presents the construction and the validation of a volumic crash detailed model of different spotwelded coupons using the finite element method. The goal of this detailed model is to provide input data for the validation of a simplified model, which will be later on implemented in the complete car model. First, by studying a weld's cross section, three different areas (spot weld, heat affected zone and basis material) have been identified and characterized using the Vickers hardness test. Moreover, the geometry of the specimen has been carefully analyzed to construct an accurate FE-model. To reflect the different mechanical properties of each zone, a simple method based on the extrapolation of the tensile strength from the Vickers hardness has been used. To compute the damage and the rupture inside the specimen, the Gurson material model implemented in the explicit time integration method "LS-DYNA3D" has been used. The global accuracy of the detailed model is checked by comparing the simulated and experimental force/displacement curves and the weld's rupture mode under a quasi-static load case of 10 mm/min. This study shows that detailed models of shear-tension, lap-shear and coach-peel specimens are validated for a mild steel.

E. H. J. Lamouroux (✉) · D. Coutellier
Laboratory L.A.M.I.H. UMR CNRS 8530,
University of Valenciennes,
59313 Valenciennes Cedex 9, France
e-mail: Emmanuel.Lamouroux@daimlerchrysler.com

N. Doelle · P. Kuemmerlen
DaimlerChrysler AG, Research and Technology,
Mercedesstrae 137, 70546 Stuttgart, Germany

Keywords Detailed modelling · Gurson damage model · Spot-weld · Quasi-static · Material identification

1 Introduction

Since many years now, a lot of effort has been done by different international associations to improve the passenger car's safety. Thus, different ratings are now employed to evaluate the ability of a car to resist to a crash impact. As a matter of fact, in order to be top ranked, each brand should improve their car's structure on the required tested area. Reproducing crash tests to study car's behaviour costs not only a lot of money but also a lot of time. In order to reduce the costs, simulation has taken an important part for some years. In fact, the development of super computers and improvements in finite element codes allow nowadays simulating a complete car crash. In terms of numerical simulation of crash behaviour, the most recent comparisons between numerical/experimental testiness have shown that the main source of results dispersion is due to a bad prediction of the mechanical behaviour and fracture of spot-welded structures or other joining techniques such as adhesive bonding, clamping or laser welding.

Many studies are available in the literature concerning the spot welding and most of them concern the fatigue's resistance through for example numerous works of Radaj [1] and Zhang [2] or the simulation of the welding process and its optimization using often the software SYSWELD+® [3].

In the complete car model, the whole frame and all the different joining techniques have to be modelled in order to represent as best as possible the reality. For crash simulation, it is very important to know how

many joints will fail and to be able to predict not only their location but also the force they can withstand. In fact, during the crash the spot weld can fracture, which induces that the complete structure will have different deformations and intrinsic mechanical properties than before the impact. Since, a car's frame contains several thousand spot-welds, it is impossible to have a detailed representation of each spot-weld according to the huge calculation time they require. One possibility for a reliable and practicable description of spot welds in the crash simulation is to developed replacement elements based on simple elements such as connector or hexa-element. To define the mechanical properties of this simplified element, the deformation and failure behaviour of the spot weld has to be characterised.

The classical way is to make numerous of experimental campaigns for different materials, thicknesses, load angles and load speeds to develop a general failure criterion leading to the creation of a simplified element. Thus, the immense number of experiments needed to validate the simplified model takes a lot of time and money. As a matter of fact, the goal of our work is to develop a method for the determination of the load-carrying capacity of the spot weld (for different material combinations and for different load conditions) using few standard experiments and detailed simulations. This procedure using simplified and detailed models is since many years widely used. For example, in 2001, using the explicit FE-code PAM-SOLID™, Markiewicz et al. [4] have identified a material behaviour law for the various zones of a spot-weld under quasi-static loadings. They analysed and studied, for a metal sheet assembly structure of 0.7 mm/0.7 mm, the rupture of spot welded tensile-shear, cross-tensile and peeling specimen using the Gurson material model. Nowadays, different activities on the topic using also the Gurson damage model and the FE-code ABAQUS/STANDARD are also running at the Fraunhofer Institute in Freiburg (Germany) [5].

To have access to the local mechanical properties of the spot-welded structures, a method based on simple tests such as micro-hardness measurements and tensile tests will be proposed. With the previous mechanical data and with the pre-processor Medina [6] a very fine numerical model composed of eight nodes elements with a length of around 0.2 mm will be constructed. In order to represent as best as possible the reality, a model of testing bench's stiffness will be also implemented in the FE-model. In the first instance the study is limited to the case of quasi-static loadings, knowing that the objective will be to predict the dynamic behaviour of structures. Using LS-DYNA3D [7] as processor and post-processor, the validation of this first method will be done for three different specimens (made of supple steel): shear-tension, lap-shear and coach-peel for three different sheet thickness combinations: 1.50 mm/1.50 mm, 1.50 mm/1.00 mm and 1.00 mm/1.00 mm.

2 Characterisation of the different components of the spot-weld

Basically, welding is a process used to permanently join two, usually metallic, components by the localized coalescence that occurs under certain combinations of temperature, pressure and metallurgy [8]. The components are welded together as a result of the heat created by electrical resistance. This is provided by the work pieces as they are held together under pressure between two electrodes. Spot welding may be performed manually or robotically and may take between 0.75 and 1 s per weld.

The range of pressure and temperature used is quiet broad, although heating and cooling are integral parts of most welding processes. The particular combination of these variables results in a unique joint in terms of material variations, potential flaws and residual stresses. Some material variations occur across a weld joint because each position in the weld is subjected to a different thermal history, with some temperatures rising above, those required for phase transformations and grain growth [8]. Residual stresses are created during welding by the solidification, phase transformation and thermal shrinkage strains associated with molten weld metal as it cools. Existing without external loading, residual stresses are self equilibrating, and often reach magnitudes of yield level. They can cause cracking and distortion in weld joints and even premature failure of structures under certain conditions [9]. To show the presence of different sub-zones along the specimen, a Vickers's hardness test combined with a microstructural observation of the specimen has been used. This step will also allow us having a precise representation of the local specimen's geometry and by the way building with accuracy the FE-model's geometry.

2.1 Local geometry of the spot-welded specimen

A cross section in the middle of a spot-welded shear-tension specimen has been done as presented in the Fig. 1. On this figure, it is possible to see not only a curvature on the top and on the bottom of the spot weld, but also one singularity on each side of the spot-weld. These notches are important since they will induce a stress concentration when the weldment will be submitted to a load. These geometrical singularities are created when the electrodes press together the two material sheets to

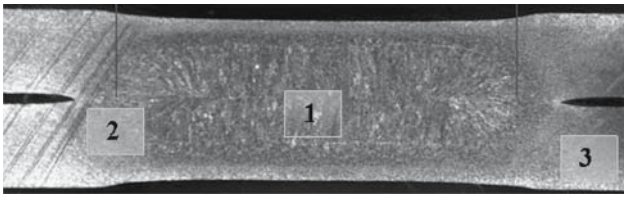

Fig. 1 Cross section of a spot welded specimen

weld them. From a structural point of view, it is possible to recognize three different phases along the specimen: the spot weld in the middle (area 1), the basis material on the edge (area 3) and in between the heat affected zone (area 2). Since this seems to be three different areas, they should have different mechanical properties. Along this cross section a Vickers hardness test will be done in order to show physically the existence of three real different sub areas.

2.2 Vickers hardness measurement

The Vickers hardness test method consists of intending the tested material with a diamond intender, in form of right pyramid with a square base and an angle of 136° between opposite faces subjected to a load of 1 N in our case. The full load is applied for 10 s. The two diagonals of the indentation left in the surface of the material after removal of the load are measured using a microscope and their average calculated. The area of the sloping surface of the indentation is calculated. The Vickers hardness is the quotient obtained by dividing the kgf load by the square area of indentation. The distance between two prints or the one between the print and the extremity of the metal sheet should be at least equal to 2.5 times the print's diagonal in order to eliminate any boundary effect [10].

In order to build later on a fine FE-modelling of the different specimens, a very detailed hardness measurement will be made to capture the change in hardness in micro-structural point of view. In fact, the distance between two prints is equal to 0.06 mm.

In the Fig. 2, the Vickers hardness is plotted for 42 measurement's points along the specimen. This shows clearly the existence of three different sub-zones (spot-weld, heat affected zone and basis material) as supposed earlier. The basis material and the spot weld can be characterized as homogenous area since the hardness seems to be constant inside a given zone. At the opposite, the heat affect zone can be characterized as heterogeneous area since the Vickers hardness changes drastically in a short distance. In the FE-model, as simplification, in each zone a constant hardness will be modelled. This means that, the heat affected zone will be considered, in first approximation, as homogeneous material.

The different approximations are represented with the bold line on the Fig. 2 and it leads to:

- Mean hardness value for the basis material: 195 HV.
- Mean hardness value for the heat affected area: 269 HV.
- Mean hardness value for the spot weld: 386 HV.
- Based on the cross section's characterization (Fig. 1), the following dimensions will be used for the finite element model representing a symmetrical thickness of 1.5 mm.
- Diameter of the spot weld: 5.6 mm.
- Diameter of the heat affected zone: 1.0 mm.

2.3 Mechanical characterization of the different spot-weld's sub-zones

As input for the finite element simulation, the strain/stress curves should be defined for each sub-zone of the specimen. The basis material's curve can be obtained from the manufacturer.

A simple method should be found to determine the characteristics for the heat affected zone and for the spot-weld. For this first detailed model's study, a simple scaling method has been chosen. In fact following the norm DIN 50150 [11] (Deutsches Institut für Normen—German institute for norms); it is possible knowing the value of the Vickers hardness to extrapolate the corresponding tensile strength for a given point. Then, by dividing the tensile strength value of the heat affected zone (respectively, of the spot weld) by the one of the basis material, a scaling factor is calculated. To obtain the stress/strain curve of the heat affected zone (respectively of the spot weld), each stress value will be multiplied by the previous calculated scaling factor.

As first approximation, the strain at rupture will be remained constant for the three subzones. This assumption is not fully in accordance with the reality since from a theoretical point of view, the strain at rupture should decrease when the Vickers hardness increases. Thus to determine properly the strain at rupture for each zone, investigations based on microspecimens are in progress to obtain an accurate value of the strain at rupture for each sub-area.

2.4 Construction of the different numerical models

The capability of the detailed model to represent accurately the reality will be tested on the shear-tension, lap-shear and coach-peel coupons (Fig. 3). The shear-tension

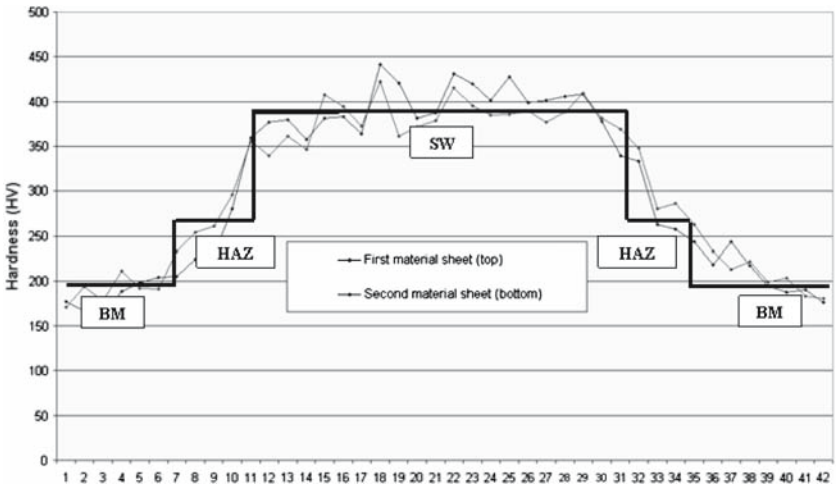

Fig. 2 Hardness diagram along a spot-welded specimen (sheet thicknesses 1.50 mm)

sample is tested using two different angles: 0 (pure shearing) and 90 (pure tensile load case). The lapshear specimen is only used to characterize the shearing behaviour of the spot weld while to characterize the tensile and bending spot-weld's behaviour, the coach-peel specimen has been employed. All numerical models of the different specimens and gage combinations have been constructed with the pre-processor Medina using eight nodes elements. For example, the shear-tension coupon's model for a symmetrical sheet thickness of 1.50 mm contains approximately 320.000 eight nodes elements. The different numerical models are presented in the Fig. 4. In order to avoid instabilities and too large modelling influences on the calculus, each sub-area of the specimen (basis material, heat affected zone and spot-weld) is modelled with elements having approximately a constant size. The shorter elements have a length of 0.20 mm and the larger one a length of 1 mm. The larger elements are of course located at the border of the specimen, far away from the "critical" areas (spot-weld, interface between the heat affected area and the spot weld or heat affected area itself) where the fracture will probably occur.

The numerical simulation will be performed using the Gurson material model, classified as *MAT*120 in *LS* − *DYNA*3*D*. As theoretical basis, the micromechanism of the ductile fracture initiation and particularly the Gurson material model will be described on the next paragraph.

3 Micromechanism of ductile fracture initiation and models of damage

Ductile fracture's phenomenon is initiated by void formation around non-metallic inclusions and second-phase particles in metal matrix that is subjected to plastic strain under influence of external loading. Size of the second phase particles and non-metallic inclusions in engineering alloys may range from approximately 0.01 m to values that by far exceed 1 m [12]. Their shape varies from spherical to lamellar or even irregular form. Depending on the size, shape and quantity of these particles as possible spots for initiation of ductile fracture, numerous models have been developed in an effort to describe this complex micromechanism. Some models evaluate a critical stress, others use a critical strain. Both type of criteria are based on the fact that a critical stress at the interface of an inclusion or in the centre of an inclusion must be exceeded to cause debonding or cracking of the particle [13].

In 1977, Gurson [14] has analysed plastic flow in porous materials supposing that the material behaves as continuum. The existence of voids is taken into account indirectly, through their average value. It has been experimentally shown that the Gurson model describes initial phase of fracture adequately, but that it is not adequate for actual behaviour of the material in subsequent phases of fracture initiation. Tvergaard and Needleman [15] have started from the Gurson model and, after certain modifications (explained later on), established the model that is more in accordance with experimental results. According to this modified Gurson–Tvergaard–Needleman (GTN) model, plastic potential is given by:

$$\phi\left(\sigma_{kk}, \sigma_M, f\right) = \frac{\sigma_e^2}{\sigma_M^2} + 2q_1 f \cosh\left(\frac{q_2 \sigma_{kk}}{2\sigma_M}\right) - 1 - (q_1.f)^2 = 0 \quad (1)$$

where σ_M denotes the actual flow stress of the material's matrix, σ_e is the von Mises equivalent macroscopic stress, σ_{kk} is the trace of the macroscopic stress tensor and $q1$, $q2$ are correlating parameters introduced

Fig. 3 Shear-tension, lap-shear and coach-peel coupons

Fig. 4 Numerical model of the shear-tension, lap-shear and coach-peel coupons

by Tvergaard and Needleman to improve the ductile fracture prediction of the initial Gurson model. The parameter $f*$ was added also by Tvergaard and Needleman to account for the accelerated damage rate associated with void coalescence, such that:

$$f^*(f, f_c, f_F, q_1) = f \text{ if } f \le f_c \quad \text{and } f_c + \frac{\frac{1}{q_1} - f_c}{f_F - f_c}(f - f_c) \quad \text{if } f > f_c \tag{2}$$

where f is the void volume fraction (or porosity), f_c is the critical value at which void coalescence occurs and f_F is the void volume fraction at which there is a complete loss of stress carrying capacity. It is of interest to note that for the absence of porosity ($f^* = 0$), the plastic potential (Equation 2) is reduced to a Von Mises yield surface.

The damage develops through the nucleation of new voids as a function of effective plastic strain and growth of existing voids according to:

$$\dot{f} = \dot{f}_{nuclearion} + \dot{f}_{growth} \tag{3}$$

with:

$$\dot{f}_{nuclearion} = D\dot{\varepsilon}_{eff}^{plastic} \text{ and} \tag{4}$$

$$D = \frac{f_n}{S_n\sqrt{2\pi}} exp\left[-\frac{1}{2}\left(\frac{\varepsilon_{eff}^{plastic} - \varepsilon_{eff}^{n}}{s_n}\right)^2\right]$$

$\dot{f}_{growth} = (1 - f)\dot{\varepsilon}_{eff}^{plastic}$ where f_n is the volume fraction of void-nucleating particles (or the total void volume fraction available for nucleation), $\varepsilon_{eff}^{plastic}$ and $\dot{\varepsilon}_{eff}^{plastic}$ represent the effective plastic strain and its corresponding rate, ε_{eff}^{n} is the mean strain at which nucleation occurs and S_n is the standard deviation of nucleating strains assuming a normal distribution.

4 Determination of specific material model's parameters

In the GTN material model, the following parameters: f_0, f_n, f_c, f_f, q_1 and q_2 are material's specific. As a matter of fact, these damage parameters should be identified for the studied material. For the time being, this parameter identification is done manually based on an inverse method using experimental results of simple tensile specimen. Using the experimental force/displacement curve of the tensile specimen, our goal is to fit as best as possible with the simulation the global shape (global stiffness, maximal stress level), the accumulation of damage (loss of stress carrying capacity) and the strain at rupture of the experimental curve. Moreover it is of importance to note that, in our version of LS-DYNA3D, the parameter ff is dependant of the element's size of the finite element model [16]. As a matter of fact, four numerical models of the tensile specimen have been done using eight node elements with, respectively, a length of 0.25 mm/0.33 mm/0.50 mm and 1.00 mm. The graphical results of this damage parameter optimization for the studied supple steel are presented on the Fig. 5, where the black curve is the experimental one and the coloured curves are the simulated one for the four different element sizes. The Gursons damage parameters ε_N and S_N are more or less constant for one material's family. For steels, in the literature the standard values for eN and SN are, respectively, 0.3 and 0.1. The previous curve shows a perfect accuracy of the simulation. In fact the damage evolution and the fracture

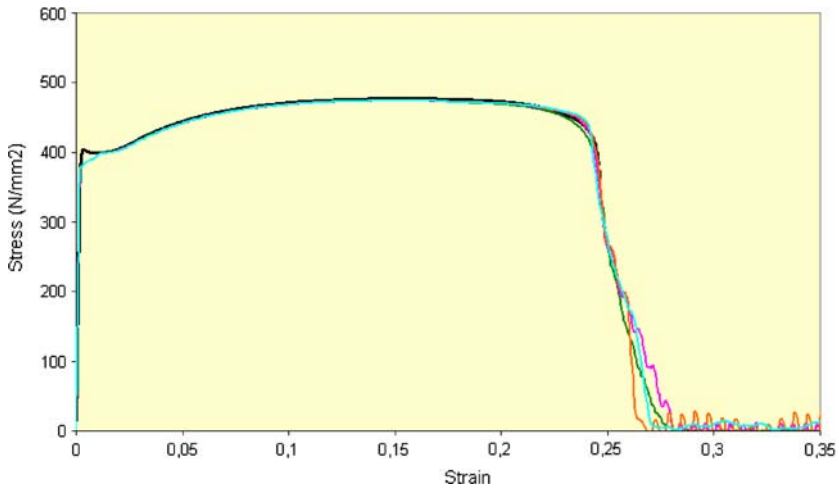

Fig. 5 Optimized damage parameters based on an inverse method using a tensile specimen

of the tensile specimen are perfectly represented in the simulation. Consequently for the studied material, the damage parameters are optimized. Using these damage parameters in the Gurson material model, the more complex specimens (shear-tension, lap-shear and coach-peel), taking also into account the accumulation of damage and the associated loss of carrying capacity of the spot weld it self, can be simulated.

5 Simulated force/displacement curves for the shear-tension, lap-shear and coach-peel coupons

As mentioned earlier, in order to validate the ability of the detailed model to represent with accuracy the reality, three combinations of sheet thicknesses and three different specimens have been simulated. As validation basis, the experimental force/displacement curve of a given specimen will be compared with the simulated one. To calculate the accumulation of damage and the specimen's fracture, the Gurson material model with the previous optimized damage parameters will be used.

The numerical simulation has been performed on a super computer which allows us modelling the whole specimen without any symmetry. The corresponding finite element models contain more than 320.000 eight nodes volumic elements for the shear-tension specimen and around 100.000 elements for the lap-shear specimen. The corresponding simulation's results for the shear-tension, lap-shear and coach-peel specimens and for the different sheet thickness combinations are plotted on the Figs. 6, 7 and 8. On these different diagrams, the bold curves represent the experiments and the normal one the simulations. The results for the shear-tension specimen tested under 90 are in red and, respectively, in black for 0. The lap-shear specimen and the coach-peel specimens are respectively plotted in blue and green. From macroscopic point of view, the simulations and the experiments are in good correlation for all specimens and all material combinations. The simulated global stiffness is in accordance with the experimental one. The simulated maximum force level that the spot weld can withstand and its corresponding displacement are obtained with accuracy compared to the experiments (deviation of approximately 5percent). It is interesting to note that for all sheet thickness combinations, the shear-tension specimen under 0 can withstand to a higher force than the lap-shear specimen than the shear-tension under 90 than the coach-peal specimen. This means that it is more difficult and it requires more energy to break a sport weld by pure shearing impacts than by pure tensile impacts. The detailed simulation represents also properly the local failure of the spot-weld. In fact, for each case, the exact spot weld's rupture mode has been obtained.

Under tensile load case, pull-out failure occurs in both experiments and simulations, while under shearing solicitation, a nugget failure (the spot-weld ruptures in its centre at the notch location) can be observed in both experiment and simulation.

6 Conclusion

Using a simple Vickers hardness test and a specimen's cross section, the mechanical behaviour of three different sub-zones existing along the spot-welded specimen (basis material, heat affected zone and spot-weld) has been identified and characterized. Using a simple scaling method based on the estimation of the local tensile strength from the Vickers hardness, the material properties have been obtained for each sub-zone of the spot-weld. The local geometry of the spot-weld itself

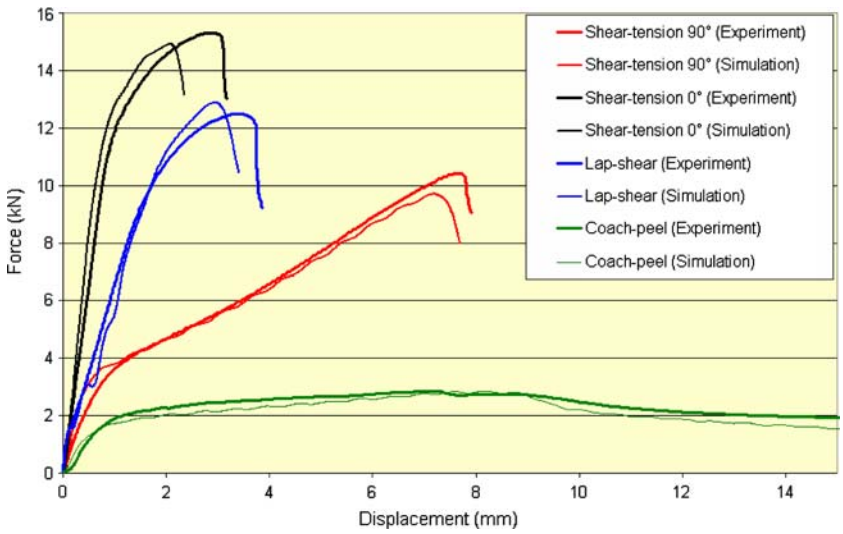

Fig. 6 Comparison of the simulated and experimental force/displacement curve for the sheet thickness combination 1.50 mm/1.50 mm

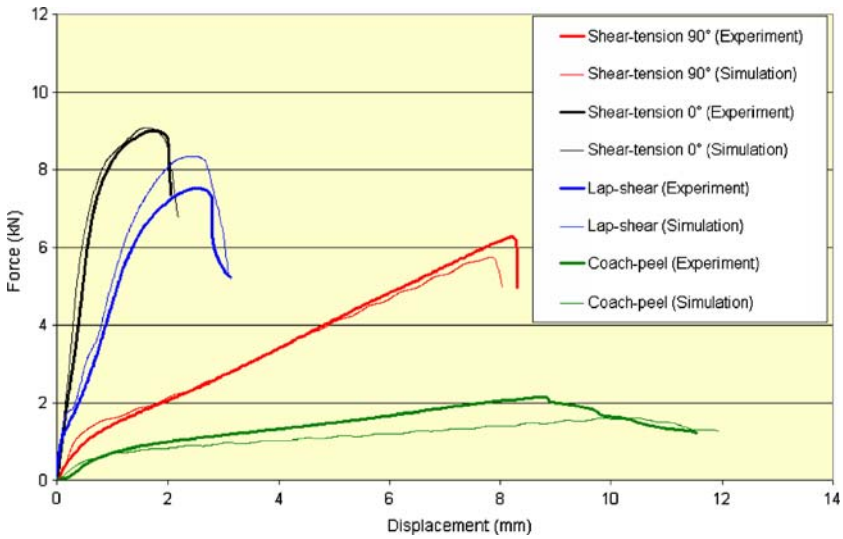

Fig. 7 Comparison of the simulated and experimental force/displacement curve for the sheet thickness combination 1.00 mm/1.00 mm

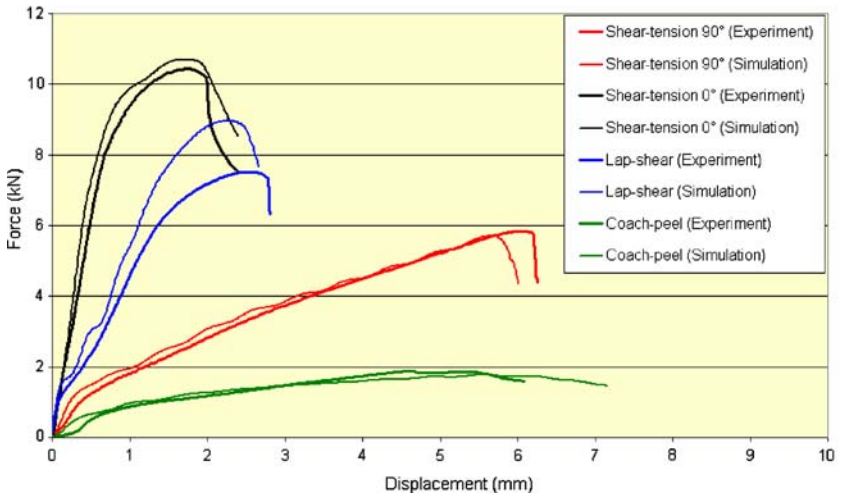

Fig. 8 Comparison of the simulated and experimental force/displacement curve for the sheet thickness combination 1.50 mm/1.00 mm

(curvature, notches, radius…) has been obtained using the previous cross-section.

With these data the three different finite element models have been built using eight nodes volumic elements. In order to obtain a good accuracy, a FE-detailed model based on elements with a length of approximately 0.2 mm has been done. To analyze the spot weld's rupture the Gurson material model has been used. In

order to compute properly the accumulation of damage and the failure, the Gurson damage parameters have been first optimized using an inverse method based on a force/displacement curve fitting from a tensile specimen. With the optimized parameters, more complex specimens (sheartension, lap-shear and coach-peel) with three different sheet thicknesses have been simulated using LS-DYNA3D.

The different simulations are in good correlation with the experimental force displacement curves in term of global stiffness, maximal stress carrying capacity and failure behaviour. As a matter of fact, the detailed model of spot-welded specimen is validated for a mild steel.

In order to generalize our approach, the same procedure will be followed for further material combinations and load cases. In a theoretical point of view, several investigations (based on mini-specimens [17]) are done to introduce a more realistic approach of the strain at rupture's evolution for an increasing Vickers hardness. Finally, in combination with experimental tests the validated detailed model of spot weld can be taken as input data for developing a simplified model. Such a simplified model which is suitable to present the failure behavior of spot weld in body in white structures was developed by Seeger et al. [18]. The methodology presented in [18] requires the characteristic force-displacement curves of each tensile-shear, lap-shear and coach-peel coupons for each material or gage combination. With the presented detailed model the number of experiments and consequently the costs can be considerable reduced.

References

1. Radaj, D.: Stress singularity, notch stress and structural stress at spot welded joints. Eng. Fract. Mech. J. **N34**, 495–506 (1989)
2. Zhang, S.: Approximate stress formulas for a multiaxial spot weld specimen. Weld. J. **N80**, 201–203 (2001)
3. SYSWELD+®. Technical report, Systus International Headquarters, 6 rue Hamelin BP 2008-16—75761, Paris Cedex 16, France
4. Ducrocq, P., Drazetic, P., Haugou, G., Berard, J.Y., Markiewicz, E., Fourmentraux, T.: Material behaviour law identification for the various zones of the spot-weld under quasi- static loadings. Int. J. Mater. Prod. Technol. **16**, 484–509 (2001)
5. Sun, D.Z., Sommer, S.: Untersuchung des einsatzes von schädigungsmodellen bei. Fraunhofer IWM (2003)
6. Medina PreProcessing. version 7.1.4 edn (2001)
7. LS-Dyna. Keyword Users Manual (2003)
8. Hill, M.R., Panontin, T.L., Nishioka, O.: Fracture assessments of welded structures. Internet Publication
9. ASM Hanbook. Welding, brazing and soldering, vol. 6 (1983)
10. Maeder, G., Barralis, J.: Précis de métallurgie, élaboration, structure, propriétés et normalisation. AFNOR Nathan (1997)
11. Deutsches Institut für Normen e.V. Prüfung metallischer Werkstoffe Umwertung von Härtewerten, din 50150 edition (2000)
12. Thomason, P.F.: Ductile fracture of metals. Pergamon, Oxford (1990)
13. Prahl, U., Dahl, W., Bleck, W., Achenbach, U., Klingbeil, S.: Fracture from defects. In: Brown, M.W., De la Rios, E.R., Miller, K.J. (eds.) Proceedings of ECF 12, pp. 877–881. EMAS Publishing, Sheffield (1998)
14. Gurson, A.L.: Continuum theory of ductile rupture by void nucleation and growth: part. J. Eng. Mater. Technol. **99**, 2–15 (1977)
15. Tvergaard, V., Needleman, A.: An analysis of ductile rupture in notched bars. J. Mechan. Phys. Solids **N32**, 461–490 (1984)
16. Fassnacht, W., Feucht, M.: Simulation der rissbildung in aluminiumgussbauteilen. Technical report, DaimlerChrysler AG (1999)
17. Yeni, C., Kocak, M., Cam, G., Erim, S.: Determination of mechanical and fracture properties of laser beam welded steel joints. Weld. J **N78**, 193–201 (1999)
18. Frank, T., Keding, B., Haufe, A., Seeger, F., Feucht, M.: An investigation on spot weld modelling for crash simulation with ls-dyna. In: LS-DYNA Users forum 2005, Bamberg, Germany. LS-DYNA Users forum (2005)